Continuous self-repair protects vimentin intermediate filaments from fragmentation

Quang D. Tran [a],[1,†] Martin Lenz,[2,3] Hugo Wioland,[1] Antoine Jegou,[1] Guillaume Romet-Lemonne,[1] and Cécile Leduc[1,‡]

[1] *Université Paris Cité, CNRS, Institut Jacques Monod, F-75013 Paris, France*

[2] *Université Paris-Saclay, CNRS, LPTMS, F-91405 Orsay, France*

[3] *Physique et Mécanique des Milieux Hétérogènes (PMMH), CNRS, Ecole Supérieure de Physique et de Chimie Industrielles de la Ville de Paris, Paris Science et Lettres Research University, Sorbonne Université, Université Paris Cité, F-75005, Paris, France*

[a] Present address: Department of Physics, Brandeis University, Waltham, MA 02453

Abstract

Intermediate filaments are key regulators of cell mechanics. Vimentin, a type of intermediate filament expressed in mesenchymal cells and involved in migration, forms a dense network in the cytoplasm that is constantly remodeled through filament transport, elongation/shortening, and subunit exchange. While it is known that filament elongation involves end-to-end annealing, it is unclear how the reverse process of filament shortening by fragmentation occurs. Here, we use a combination of *in vitro* reconstitution probed by fluorescence imaging and theoretical modeling to uncover the molecular mechanism involved in filament breakage. We first show that vimentin filaments are composed of two layers of subunits, half of which are exchangeable and half of which are immobile. We also show that the exchangeable subunits are tetramers. We further reveal a mechanism of continuous filament self-repair in which a soluble pool of vimentin tetramers in equilibrium with the filaments is essential to maintain filament integrity. Filaments break as a consequence of local fluctuations in the number of subunits per cross-section induced by the constant subunit exchange of tetramers. We determine that a filament tends to break if about four tetramers are removed from the same filament cross-section. Finally, we analyze the dynamics of association/dissociation and fragmentation to estimate the binding energy of a tetramer to a complete versus a partially disassembled filament. Our results provide a comprehensive description of vimentin turnover and reveal the link between subunit exchange and fragmentation.

Keywords: Plakins, Plectin, Cytoskeleton, Rheology, Binding kinetics

SIGNIFICANCE STATEMENT

Intermediate filaments, including vimentin, are a key component of the cytoskeleton, which is essential for cell mechanics. Inside the cell, vimentin forms a dense network that is constantly remodeled to fulfill its functions. In particular, the filaments elongate and fragment, but the molecular mechanism involved in this breakage was unknown. Here we show that fragmentation is a consequence of the constant exchange of subunits along the filament length, which could locally weaken the filament. Our results provide a physical understanding of the mechanisms involved in regulating filament length, a feature that is

† quangtran@brandeis.edu

‡ cecile.leduc@cnrs.fr

essential for determining the dynamic organization of the network in both healthy and diseased cells in which intermediate filament assembly is disrupted.

INTRODUCTION

Intermediate filaments (IFs) are one of the three major components of the cytoskeleton, along with actin filaments and microtubules, and play a critical role in determining cell shape and cell mechanics. In particular, IFs help preserve cell integrity as they are essential for cells to withstand large deformations Hu et al. (2019), Latorre et al. (2018), Nagle et al. (2022). In addition to their well-known mechanical functions, IFs have also been implicated in other cellular functions such as signaling, division, polarity and migration Patteson et al. (2020), often through their interplay with the other types of cytoskeletal filaments Huber et al. (2015), Leduc and Etienne-Manneville (2015). Many pathologies have been linked to mutations in IF proteins that result in disruption of IF assembly or remodeling Omary et al. (2009). Despite these important cellular functions, the mechanisms involved in the dynamics of IF assembly/disassembly are much less understood than those pertaining to F-actin and microtubules.

IFs form a large and heterogeneous family divided into six main classes. Vimentin, a class III IF, is predominantly expressed in cells from mesenchymal origin and its expression level is commonly used as a marker of the epithelial-mesenchymal transition Kalluri and Weinberg (2009). Vimentin filaments form a dense and interconnected network that expands from the nucleus to the plasma membrane, and whose dynamic remodeling is essential for its cellular functions. In cells, filament assembly occurs through end-to-end annealing Çolakoğlu and Brown (2009) and filament disassembly is believed to be regulated by post-translational modifications (PTMs) such as phosphorylation Eriksson et al. (2004), Inagaki et al. (1987), Snider and Omary (2014). Indeed, phosphorylation of vimentin reduces the amount of positive charges in the head domain, thus destabilizing internal interactions and leading to filament disassembly Eriksson et al. (2004), Kraxner et al. (2021). The *in vitro* reconstitution of vimentin filaments with purified proteins has provided additional insights into the mechanism of filament assembly Brennich et al. (2011), Hémonnot et al. (2015), Herrmann et al. (1996), Lopez et al. (2016), Nöding et al. (2014), Schween et al. (2022), Sokolova et al. (2006), Winheim et al. (2011). These experiments showed that the initial

step of assembly relies on the lateral association of apolar tetramers to form short filament precursors called unit-length filaments (ULFs). ULFs then undergo end-to-end annealing for further longitudinal elongation Herrmann and Aebi (2016). Unlike actin and microtubules, there is no polymerization by the addition of subunits at the filament ends. Once assembled, vimentin filaments are very stable; they can be kept at room temperature for more than a week. The only way to disassemble them is to greatly decrease the ionic strength (<20 mM) or add denaturing reagents Herrmann and Aebi (2016).

Although they are very stable, we have recently shown that vimentin filaments can spontaneously fragment in the absence of severing proteins or PTMs Tran et al. (2023). We estimated the mean bond breaking time between successive ULFs to be ∼18 h, which is of the same order of magnitude as the filament breaking time observed in cells Hookway et al. (2015). However, the molecular mechanism involved in this filament breakage is unknown. Here we propose that the local dissociation of subunits from the lattice would weaken the filament and induce filament breakage. Indeed, the incorporation and loss of subunits along pre-existing filaments has been reported in cells Coleman and Lazarides (1992), Ngai et al. (1990) and has been shown to occur in parallel with filament annealing Çolakoğlu and Brown (2009), but it remains unclear whether the two types of filament dynamics are related to each other. Subunit exchange has been reconstituted *in vitro* using purified vimentin Nöding et al. (2014). However, characterization of the subunit loss from the lattice was missing, preventing estimation of the total number of subunits per cross-section and its fluctuations. Furthermore, the existence of subunit exchange implies that there is a pool of soluble subunits in equilibrium with the filaments as observed in the cytosol (∼1-3% of total vimentin for cells in culture Soellner et al. (1985), but this pool has been found to be negligible *in vitro* Sokolova et al. (2006) or could not be detected in the absence of phosphorylation Eriksson et al. (2004). In the standard model of IF assembly, all tetramers self-assemble into ULF within seconds when filament elongation is initiated upon salt addition, implicating the absence of a vimentin soluble pool Herrmann and Aebi (2016). Hence, there are still contradictory observations that need to be reconciled to fully understand the assembly model of vimentin, and how it is related to subunit exchange. A complete description of vimentin dynamics is required to understand how the filament length and the soluble pool of subunits are inherently regulated, a feature that is crucial to determine the network architecture in cells and how it can be impacted in diseases.

Here, we elucidate the molecular mechanism responsible for vimentin filament fragmentation using *in vitro* single-filament fluorescence studies coupled with theoretical modeling. We show that filament breakage is a consequence of the constant subunit exchange along the filament length. Subunit exchange can cause local fluctuations in the number of tetramers per cross-section, weakening the filament and thereby inducing fragmentation. Overall, we show that continuous self-repair of the filament by subunit exchange is essential to ensure its structural integrity, a key feature for its length regulation over long time scales.

RESULTS

Vimentin subunits spontaneously self-renew along filaments

We propose that filament fragmentation results from a local transient dissociation of subunits that would weaken the filament. To test this hypothesis, we first quantified the effect of subunit association/dissociation along the filament over 24 h, which is the time scale at which fragmentation occurs under our experimental conditions Tran et al. (2023). We thus mixed two populations of filaments: one pre-assembled from recombinant vimentin fluorescently labeled on cysteine-328 and one from unlabeled vimentin Petitjean et al. (2024), Tran et al. (2023), Winheim et al. (2011)(Fig. 1A). We imaged the filaments at several time points after mixing over 24 h, and confirmed that they continued to elongate by end-to-end annealing, as shown by the succession of bright and dim segments along the filaments and continuous increase in filament length (Fig.1B, Fig. S1A). We also verified that when fluorescent filaments were not mixed with unlabeled filaments, the level of fluorescent intensity remained constant over time (Fig. 1C, control), indicating that the linear density of vimentin subunits per length remained constant on average during the assembly process.

If all subunits were able to associate/dissociate, we would expect that for a 1:1 labeled:unlabelled mixture that has reached a steady state, the intensity of the labeled segments would be divided by two and the intensity of the whole filament would become homogeneous. Instead, the two populations remained non-homogeneous after reaching a steady state (Fig. 1B, Fig. S1A). We assessed the extent of subunit exchange by quantifying the pixel fluorescence intensities along the filaments with bright and dim segments, then fitting the distribution with a double Gaussian, and finally normalizing the peak intensities

corresponding to initially unlabeled and labeled segments by the mean intensity of labeled filaments before mixing (Fig S1B, Methods). We observed that the normalized intensity of the labeled segments reached a steady state after 21 hours (Fig. 1C), with a value of $\sim$0.75 for a 1:1 labeled:unlabeled mix, and $\sim$0.55 for a 1:9 labeled:unlabeled mix at steady state (Fig. S1C). These results indicate that only half of the subunits are exchangeable. Finally, by modeling the subunit exchange along the filaments using a simple 2-state model (see the theory part in the Supp Info), we extracted the dissociation rate of the subunit from the filament by the exponential fitting of the curves in figure 1C, and obtained $k_{\text{off}} = 0.2 \pm 0.1$ h^{-1} (mean $\pm$ SD, $N = 3$ independent repeats). We assumed in the model that the subunits were tetramers, which we verified in experiments presented later in this paper. Taken together, our results confirm that there is incorporation and loss of vimentin subunits in already formed filaments, and also show that subunit association and dissociation are counterbalanced. Furthermore, our results reveal that there is a core of non-exchangeable subunits corresponding to about half of the subunits composing the filaments.

Characterization of vimentin soluble pool

Vimentin filaments spontaneously renew their constituents by association/dissociation of subunits along their length, implying that there is a soluble pool of vimentin in equilibrium with the assembled filaments. However, the amount of vimentin subunits in the solution is so low that it has never been detected at physiological ionic strength (100 mM KCl). To be able to detect the soluble pool of vimentin, we first separated polymerized and unpolymerized vimentin by centrifugation at 140,000 $\times g$ for 15 min and concentrated the supernatant by a factor 10 using centrifugal filter units. We then measured the concentration of soluble vimentin in the supernatant by quantification of band intensity on SDS-PAGE gels (see methods). Starting from filaments assembled at 0.2 mg/mL (2 hours at 37 °C), we measured a soluble pool of $(5 \pm 2.5) \cdot 10^{-3}$ mg/mL, corresponding to 2% of total vimentin (Fig. 1D-E). We also compared the concentration of soluble vimentin of both labeled and unlabeled filaments and found no significant difference, indicating that fluorescent labeling of vimentin has little effect on their association/dissociation properties (Fig. 1D-E). Next, we investigated whether a solution of tetramers at the concentration of the soluble vimentin could form filaments on its own using super-resolution microscopy. We performed STochas-

tic Optical Reconstruction Microscopy (STORM) imaging of a solution of 5×10^{-3} mg/mL vimentin, 20% labeled with AF-647, assembled for 6h at 37 °C and then non-specifically bound to a clean coverslip. We did not observe any filaments or filament precursor ULFs, in contrast with control conditions where vimentin filaments were either fully assembled (0.2 mg/mL assembled for 1h, 40X diluted) or assembled as ULF precursors (0.2 mg/mL assembled for 2 s, 40x diluted)(Fig. S2). Overall, our results show that there is a soluble pool of vimentin in equilibrium with filaments and that the concentration of the soluble pool ($\sim 5 \times 10^{-3}$ mg/mL for filaments assembled at 0.2 mg/mL) is so low that it will not form filaments on its own after 6 hours in the presence of salt.

Dilution induces both filament thinning and fragmentation

Association/dissociation of vimentin subunits along filament length is taking place in parallel with filament end-to-end annealing/fragmentation. As dilution of preassembled filaments shift the balance between elongation and fragmentation towards filament shortening by limiting annealing Tran et al. (2023), we wanted to assess whether this would also shift the balance between subunit association and dissociation in favor of dissociation, given that the soluble pool of vimentin would be diluted. We diluted pre-assembled fluorescently-labeled filaments (0.2 mg/mL, 2h at 37 °C) at different dilution ratios and incubated them further at 37 °C for up to 6h (Fig. 2A). We imaged the filaments at different time points after dilution and used the mean fluorescence intensity per filament as a measure of the number of subunits per cross-section (Fig. 2B-C). Filament intensity decreased after 1:200 and 1:500 dilution, with little difference between dilution ratios, while remaining constant over time for undiluted filaments (Fig. 2D). The intensity of the filaments reached a saturation value of ∼75% of its initial value after 6 h in the case of a 1:200 dilution, indicating that a new equilibrium between the soluble pool and the polymerized filaments had been reached. At a dilution of 1:500, the filaments became so short after 2 hours that neither length nor intensity could be measured. We verified that the labeling ratio of vimentin did not affect the subunit dissociation (Fig. S3), indicating that subunit exchange is not impacted by fluorescent labeling of the subunits. As previously observed Tran et al. (2023), the mean filament length decreased with time after dilution due to fragmentation, with greater shortening at the higher dilution ratio of 1:500 (Fig. 2E). These results show that filament dilution induces both filament

fragmentation and a decrease in the number of subunits per cross-section, which we refer to as filament thinning. The question arises as to whether the dissociation of subunits could destabilize the integrity of the filament and lead to its fragmentation.

Addition of soluble tetramers protect diluted filaments from fragmentation

To assess whether dissociation of subunits causes filament fragmentation, we performed experiments in which the pre-assembled filaments were diluted in a solution of tetramers (Fig. 3A). The idea was to restore the net association of vimentin subunits to counteract the dissociation of subunits along filaments induced by the low concentration of soluble vimentin after dilution, thereby restoring the equilibrium between a soluble pool of vimentin and filaments. If the integrity of filaments is preserved, they might be less subject to fragmentation. We diluted pre-assembled fluorescently-labeled filaments at ratios of 1:200 and 1:500 in solutions of fluorescently-labeled vimentin tetramers at 0.1×10^{-3}, 1×10^{-3} and 5×10^{-3} mg/mL, and incubated them further for up to 6h at 37 °C (Fig. 3A). We showed that tetramers cannot self-assemble at these concentrations of soluble vimentin (Fig. S2). We imaged the filaments at different time points after dilution and quantified both the mean fluorescence intensity of the filaments and their mean length (Fig. 3C-F). Providing filaments with 0.1×10^{-3} and 1×10^{-3} mg/mL tetramers was not sufficient to fully counteract subunit dissociation and filament fragmentation. On the contrary, the presence of 5×10^{-3} mg/mL tetramers, previously identified as the concentration of the soluble vimentin pool for filaments assembled at 0.2 mg/mL (Fig. 1E), prevented both effects (Fig. 3C-F). This indicates that the presence of 5×10^{-3} mg/mL tetramers allows their association to balance their dissociation from the filaments and prevent fragmentation, resulting in a constant mean filament fluorescent intensity and mean filament length over time (Fig. 3C-F). To further verify that filament dissociation and rescue was not an artifact coming for vimentin fluorescent labeling, we repeated the rescue experiments using unlabeled filaments diluted in a solution of labeled tetramers. Filament intensity increased over time after dilution, confirming that unlabeled tetramers dissociated from filaments and were replaced by labeled ones (Fig. S4). Dilution of green filaments in a solution of red tetramers revealed that the red tetramers had replaced ∼25% of the green tetramers after 6h incubation, as shown by the anticorrelation of the red and the green signal along the filaments (Fig. S5).

Taken together, our results show that the soluble tetramers maintain filament integrity and that subunit dissociation induces fragmentation. We show that the two disassembly mechanisms - filament fragmentation and subunit dissociation - are indeed coupled.

Next, we asked whether the dilution-induced thinning of the filaments was fully reversible, *i.e.*, whether the filaments could recover the initial number of subunits per cross-section before dilution. After 3 hours of dilution, we re-injected tetramers to the partially disassembled filaments and imaged the filaments at several time points after tetramers addition (Fig. 3G-H). After adding tetramers to reach a final concentration of 10^{-3} mg/mL, filaments quickly recovered their initial fluorescence intensity, and therefore the number of subunits per cross-section, within a few minutes (Fig. 3I), indicating that filament thinning is reversible. By modeling the mass conservation along the filaments using a simple 2-state model (see theory in the Methods section), we extracted the association rate of a subunit into a filament: $k_{\mathrm{on}} = 9 \times 10^3$ (mg.mL^{-1} h)$^{-1}$ = 0.14 μM^{-1}s^{-1} (0.06 to 0.28, 95% CI) by the exponential fitting of the curve in figure 3I. Note that we do not expect the equilibrium concentration of the soluble pool to equal the dissociation constant ($k_{\mathrm{off}}/k_{\mathrm{on}}$) because it depends on the number of binding sites, along the shaft of the filament, which depends on the history of the sample (see theory in the Methods section.)

Direct observation of subunit dissociation from the filaments after dilution

Using ensemble measurements, fixing filaments at different time points, we showed that filament dilution induces subunit dissociation, which can be compensated by subunit association if there are enough subunits in the soluble pool. We wanted to confirm these results with direct observations of subunit dissociation at the level of individual filaments, followed over time. We designed an *in situ* assay to monitor the changes in the fluorescence intensity of individual AF488-labeled-vimentin filaments anchored by antibodies to the surface of a flow chamber over time using Total Internal Reflection Fluorescence (TIRF) microscopy (Fig. 4A). After flowing and incubating the pre-assembled filaments in the flow chamber, we rinsed with the assembly buffer only, to completely remove the unbound filaments and the soluble pool of vimentin. The chamber was then sealed and placed on a microscope stage with temperature maintained at 37 °C. In a standard chamber (with a height H ∼100 μm), we observed that the fluorescence intensity of the filaments decreased and reached a plateau

at ∼45% after 6 h (Fig. 4B-C), indicating that subunits dissociated from the filaments until a new dynamic equilibrium was reached. This plateau value was below the minimum plateau value of ∼75% observed in bulk experiments (Fig. 2D), suggesting that surface binding of filaments can alter the dynamic properties of their subunits. We verified that photobleaching was negligible as the same number of laser illuminations used to image the control filaments for 6 h only resulted in less than 5% intensity loss (Fig. S6). Further, the dissociation of subunits from vimentin filaments was unaffected when changing the fluorescence labeling fraction, buffer solutions, or the density of antibodies on the substrate (Fig. S7A-C). This last observation indicates that the available surface-anchored antibodies had a negligible effect on the pool of soluble vimentin. The saturation of the fluorescence intensity after 6h suggested that the dissociated subunits had formed a new soluble pool in equilibrium with the attached filaments. To test this hypothesis, we performed a second rinse of the chamber to remove all newly dissociated subunits 6h after the first rinse (Fig. S8A). The second rinse induced a further decrease in normalized filament intensity (Fig. S8B), confirming that the first plateau was set by the equilibrium between the soluble pool and the filaments. This dynamic equilibrium also implied that the fluorescence plateau should be set by the volume of the flow chamber for a constant concentration of filaments attached to the surface. To test this hypothesis, we repeated the *in situ* dissociation assay using flow chambers of different heights ($0.1H$ and $4H$) (Fig. 4B). Lower-volume chambers resulted in a higher equilibrium intensity plateau while higher-volume chambers resulted in a lower intensity plateau (Fig. 4C). The relationship between the chamber height and the plateau value was well predicted by theoretical modeling (Fig. S9), confirming that the chamber volume sets the concentration of the soluble vimentin and therefore the level of filament dissociation. Moreover, by fitting the fluorescence intensity decay over time following our theoretical description (see Supp Info), we estimated the subunit dissociation rate $k_{\text{off}} = 0.23 \pm 0.08$ h^{-1} (mean ± SD, $N = 3$ independent repeats), in good agreement with the value provided with bulk experiments; $k_{\text{off}} = 0.2 \pm 0.1$ h^{-1} (Fig. 1). Interestingly, filaments attached on the surface rarely displayed fragmentation after thinning. This may be due to a stabilizing effect induced by the antibodies to which the filaments are attached or to the fact that filament breakage is more difficult to detect since the filament tips remain attached to the surface at a distance below the resolution of standard fluorescence microscopy.

Next, we tested whether we could also prevent filament thinning in the *in situ* assay,

as in bulk experiments, by flowing new tetramers after flushing out the soluble pool (Fig. 4D). While the addition of 0.1×10^{-3} mg/mL tetramers slowed down the global subunit dissociation without stopping it, a solution of 10^{-3} mg/mL was sufficient to maintain filament integrity, as filament intensity remained constant throughout the experiment (Fig. 4E). Surprisingly, this tetramer concentration is below the concentration necessary to prevent filament fragmentation after dilution in bulk experiments (Fig. 3D,F), suggesting that filament binding to the surface modifies the properties of the filament. On the contrary, reinjection of tetramers after thinning led to only a partial rescue of filament integrity (Fig. S10), unlike when the filaments are free to move in solution (Fig. 3I). Altogether, fixation of vimentin filaments on a substrate allowed direct observation of the mechanism of self-repair at the single filament level and confirmed bulk experiments, but also showed that the attachment of vimentin filaments on the surface impacts the total filament turnover as compared to freely diffusive filaments in solution.

The oligomeric state of the exchanged vimentin subunits is the tetramer

Finally, we wanted to uncover the oligomeric state of the subunits in the soluble pool. Previous studies showed that vimentin phosphorylation induces filament disassembly and that the exchanged subunits are tetramers Eriksson et al. (2004). Here, we wanted to investigate whether the subunits in equilibrium with non-phosphorylated filaments are also tetramers using single-molecule experiments. Using the same standard flow chamber as in TIRF experiments in Fig 4, we immobilized labeled vimentin filaments on a substrate, rinsed the unbound filaments and subunits out of the chamber, sealed the chamber, and incubated it for 60 minutes to enable partial dissociation of subunits from the filaments. Using a microscope with single molecule fluorescence sensitivity, and a high-power laser illumination setting, we were able to observe multiple fluorescent vimentin subunits diffusing in the chamber. In particular, we focused on the subunits that attached to the substrate and got photo-bleached (Fig. 5A-B). Fluorescence quantification showed that these subunits (with 15% labeling fraction) had mostly 1 bleaching step and up to a maximum of 2 steps, corresponding to 1 fluorophore or 2 fluorophores bleaching. Next, we immobilized fluorescently labeled vimentin tetramers on a substrate, and also performed photo-bleaching experiments on them. The tetramers with ∼15% labeling fraction showed similar distribu-

tion of bleaching steps as the subunits in the previous experiment (Fig. 5C), indicating that the exchanged subunits are in tetrameric form. As a positive control, we verified that when the labeling fraction of the tetramers is increased to 50%, the number of bleaching steps also increases with an average of 2 bleaching steps, and up to 4 bleaching steps (Fig. 5D). We also showed that the lifetime of a subunit binding on the substrate is longer than its average bleaching time, which ruled out the possibility of subunits/tetramers unbinding from the substrate during the photo-bleaching experiment (Fig. 5E). These results show that the dissociated subunits are tetramers and that the soluble pool of vimentin in equilibrium with the filaments is made of tetramers.

Kinetic scenario for filament fragmentation

The quantification of the kinetic parameters pertaining to the association and dissociation of individual subunits allows us to investigate the relationship between these processes and filament fragmentation. We propose that while the detachment of a single subunit does not compromise the integrity of the filament, the simultaneous absence of multiple neighboring subunits can. In a first simple theoretical model, we consider only a cross-section of the filament, which can contain a maximum of 5 mobile tetramers in addition to its 5 core tetramers (Fig. 6A). This is consistent with the results presented in figures 1 and S1, which indicate there is a core of ∼50% non-exchangeable subunits and with the latest structural data on vimentin showing that there are 10 tetramers per cross-section Eibauer et al. (2024). We assume that each subunit stochastically associates to and dissociates from the filament independently from the others, as a first approximation, following the rates k_{on} and k_{off} measured above. As soon as a critical number of subunits R are removed from the same cross-section, the filament fragments instantly at this location. By applying first-passage-time theory to a filament in equilibrium with a solution containing a concentration $c = 100$ nM (5×10^{-3} mg/mL) of soluble tetramers (Fig. 1D-E), we compute the average time required for such a fragmentation event to occur, as a function of R Van Kampen (1992)(see Supp Info). We find that the best match to our previous experimental estimate of this time, namely 18 h Tran et al. (2023), is obtained for $R = 2$, and yields a fragmentation time of 63 h.

While this first model yields a fragmentation time in order-of-magnitude agreement with

experimental measurements, it also conflicts with our observations in one crucial way. Indeed, the value $R = 2$ implies that a stable filament has at most one mobile subunit missing from each of its cross-sections. This suggests that throughout the disassembly of a collection of fully labeled filaments, no filament with a fluorescence level I_{high}/I_0 lower than 90% can be observed. By contrast, in Fig. 3D we observe fluorescence levels as low as 75%, suggesting that filaments with 2 to 3 missing subunits should still be stable (Fig. 6B). To reconcile our model with this observation, we note that a mobile subunit in a full filament is surrounded on all sides by other mobile subunits, and that the resulting binding energy is likely to stabilize it. By contrast, as soon as the filament starts losing some of its mobile subunits, the remaining ones tend to lose some of that stabilization, which facilitates their departure from the filament. As a coarse model of this facilitation, we propose that the dissociation of the first subunit in a cross-section proceeds with the rate $k_{\text{off}} = 0.2\ \text{h}^{-1}$ that we previously estimated (Fig. 1C) for the exchange of subunits between a fully assembled filament and the surrounding solution. Subsequent dissociation events, however, proceed at a faster rate $k_{\text{off}} \times e^{\Delta\epsilon/k_{\text{B}}T}$, where $\Delta\epsilon$ denotes the difference in binding energy between a fully stabilized and a less-stabilized subunit, and where $k_{\text{B}}T$ is the thermal energy. Assuming $R = 4$ compatible with the 75% intensity level in Fig. 3D, we find that this model achieves a mean fragmentation time of 18 h for a stabilization energy $\Delta\epsilon = 4.2\ k_{\text{B}}T$, although choosing $R = 3$ or $R = 5$ each change this estimate by less than 1 $k_{\text{B}}T$. This value of $\Delta\epsilon$ can be interpreted as an estimate of the difference of binding energy between a tetramer that is incorporated in a fully assembled filament, and the binding energy for the same tetramer in a configuration where some of the neighboring tetramers have already been removed.

DISCUSSION

Here, we identify the molecular mechanism responsible for filament fragmentation. First, we identify the existence of a soluble pool of vimentin that is in equilibrium with the assembled filaments. By tuning the concentration of this soluble pool, it is possible to tune both the number of subunits per cross-section and filament length. While removing the soluble pool induces both filament thinning and fragmentation, the supply of tetramers allows the filament to go back to its original state. These results indicate that the soluble pool allows the filaments to be constantly repaired, linking the two processes of subunit exchange and

filament fragmentation.

The protective effect of soluble subunits on filaments qualitatively suggests that there exists a relationship between the dissociation of mobile subunits and the loss of filament stability. Quantitatively, we interpret the discrepancy between the individual subunit dissociation rate and the comparatively slow filament fragmentation rate to gain insights into the physics underlying this fragmentation. Our results thus suggest that the detachment of multiple neighboring subunits is required for fragmentation. Here, we develop a theoretical approach that directly exploits dynamical observations and thus yields insights that are distinct from and complementary to those accessible to structural studies. Our approach robustly rules out a fragmentation mechanism wherein the mobile subunits would be decoupled from one another. We are confident that this conclusion would not change significantly even if we were to refine our admittedly coarse model of the filaments' fragmentation geometry. Indeed, any such change would only affect the combinatorial prefactors involved in our transition rates by factors of order one, which would fail to allow for stable filaments with three missing mobile subunits as observed in Fig. 3. Our second, more sophisticated, theoretical model introduces the possibility that the second, third, etc. subunits are easier to remove than the first. It furthermore indicates that the binding energy of each of these subsequent subunits is smaller than that of the first by about 4 $k_{\mathrm{B}}T$, consistent with the idea that this binding is mediated by, e.g., electrostatic interactions or hydrogen bonds. We may further estimate the subunits' binding energies by interpreting their dissociation time $1/k_{\mathrm{off}}$ as the time required for a diffusing rod of diameter $d = 2$ nm and length $l = 50$ nm to jump over an energy barrier whose height ϵ equals the subunits' binding energy with the rest of the vimentin lattice. This simple model implies $\epsilon = k_{\mathrm{B}}T \ln(\frac{\ln(2l/d)+1/2}{4\pi}\frac{k_{\mathrm{B}}T}{\eta l d^2 k_{\mathrm{off}}})$, where $\eta = 10^{-3}$ Pa.s is the viscosity of water. Numerically, this expression yields a binding energy of a mobile subunit fully surrounded by other mobile subunits of the order of $\epsilon \simeq 26\, k_{\mathrm{B}}T$. This energy is lowered by an amount of the order $\Delta\epsilon = 4\, k_{\mathrm{B}}T$ when one of these surrounding subunits is removed. While our model makes the simplifying assumption that the removed subunit is in the same filament cross-section as the subunit of interest, similar conclusions could be drawn from a model where the subunits' neighbors in the longitudinal direction are removed. Our value of $\Delta\epsilon$ should thus be understood as a rough first estimate to be refined as the geometry of the fragmentation problem becomes better understood.

Previous bulk experiments have shown that the way vimentin filaments are assembled

(kick-start vs dialysis) has an impact on the subunit exchange Nöding et al. (2014). "Kick-start" implies that the filament assembly is triggered by the addition of 100 mM KCl in one shot, whereas "dialysis" implies that the concentration of salt increases progressively during dialysis. A slow assembly has been shown to decrease the variability of the number of subunits per cross-section along filaments of filaments called polymorphism Herrmann et al. (1996). We quantified the impact of the assembly method on the subunit dissociation in the *in situ* assay and observed that filaments which are less polymorphic display slower dissociation (Fig. S7D). This is in agreement with the fact that tetramers which have fewer neighbors are more susceptible to detaching. More experiments would be necessary to characterize in more detail the difference in terms of binding energy between polymorphic filaments and filaments assembled by dialysis. For example, single-molecule experiments could be performed using optical tweezers to measure the force necessary to remove a tetramer from the filament shaft, as it has been quantified for microtubules Kuo et al. (2022). The impact of filament thinning after dilution or of phosphorylation on this removal force could also be tested.

The soluble pool of vimentin tetramers in equilibrium with the filaments allows the filaments to maintain their integrity. In a cellular context, there might be yet unidentified proteins that interact with soluble vimentin subunits and sequester them. Sequestration of subunits would prevent continuous self-repair of the filaments and therefore promote filament fragmentation, which could be a way to regulate filament length. Subunit sequestration has been shown to regulate the dynamics of other types of cytoskeletal filaments Belmont and Mitchison (1996). In the same line of thought, the recruitment of proteins at the surface of the filaments may also stabilize or destabilize the filaments by modulating the subunit association/dissociation rates. Another way to regulate filament subunit exchange in cells is to modify the subunit association/dissociation rates by modifying the binding energy between the subunits. Previous works have shown that vimentin phosphorylation triggers filament disassembly Eriksson et al. (2004), Inagaki et al. (1987), Snider and Omary (2014). Eriksson et al showed that vimentin phosphorylation increases the soluble pool of tetramers *in vivo* and *in vitro* (although the *in vitro* soluble pool in the absence of phosphorylation was previously undetectable), suggesting that vimentin phosphorylation changes the equilibrium constant of subunit exchange towards a higher off-rate Eriksson et al. (2004). More work would be necessary to characterize the effect of phosphorylation, quantify the modified on-

and off-rate, and verify whether phosphorylation favors filament thinning and fragmentation. Other PTMs could also be investigated such as S-gluathionylation which has been shown to induce vimentin fragmentation Kaus-Drobek et al. (2020), or as oxidation which induces vimentin remodeling into biomolecular condensates Martínez-Cenalmor et al. (2024). Finally, another way to tune IF length and network topology through variation of subunit association/dissociation would be to change the composition of the filaments. IFs represent a large family of proteins (> 70 genes in humans). Depending on the cell and tissue type as well as differentiation and stress, different IF proteins can coassemble within the same filament leading to complex IF composition Leduc and Etienne-Manneville (2015). Subunit exchange could be a way to modify filament composition progressively without completely disassembling the IF network.

Vimentin filaments, whether freely diffusing in solution or bound to a surface, show little difference in the rate of dissociation of tetramers from the filament. However, tethering the filaments to the surface does affect the overall turnover. Attached filaments display stronger thinning after removal of soluble vimentin and require a 5-fold lower concentration of tetramers in solution to maintain their integrity compared to filaments in solution. Besides, thinning can only be partially reversible for filament attached to the surface (Fig. S10). We believe that this difference between bulk and *in situ* experiments could be induced in part by stabilization effects induced by anchoring filaments to the surface via antibodies. Binding to the surface may maintain the integrity of filaments by keeping together fragments that would otherwise drift away from one another. In addition, anchoring the filament may induce internal reorganization of the filament, as previous studies have shown that vimentin filaments flatten when attached to a surface Lorenz et al. (2019). Flattening may impact the coupling between the filament subunits, and expose the core of the filaments. Given that the lateral bonds between the subunits determine the mechanical properties of the filaments, it may be possible to regulate filament turnover in cells by constraining the vimentin filaments.

Experiments on purified vimentin filaments showed single filaments can be stretched up to 350% without breakage Block et al. (2017). These remarkable mechanical properties are based on the hierarchical organization of the tetramers within the filaments. For strain up to $\sim$100%, vimentin stretching results from the unfolding of its alpha-helices Block et al. (2018), Forsting et al. (2019), Lorenz et al. (2019), Nunes Vicente et al. (2022). Interestingly, vimentin filaments keep softening upon repeated cycles of stretching and relaxation,

therefore filament mechanics depends on the strain history. However, the remaining plastic strain is negligible as filaments recover their initial length after relaxation Lorenz et al. (2023). It would be interesting to probe the impact of filament stretching on the association/dissociation rate of tetramers. One could also test whether subunit exchange could reset filament mechanics by providing new tetramers to stretched filaments and allowing filament renewal by incubation at 37 °C for a few hours. This partial reset of filament could also be relevant in cells where the soluble pool of vimentin can be regulated. Thus, the self-repair mechanism uncovered in this work may have further implications for cellular functions implicating vimentin such as cell resilience, resistance to large deformations Hu et al. (2019) or mechanosensitivity Ndiaye et al. (2022). Interestingly, the soluble pool of cellular vimentin has been shown to be sensitive to stimuli that alter cellular tension and morphology Murray et al. (2014).

Filament self-repair has been observed in another type of cytoskeletal filament, namely microtubules. Recent works have shown that tubulin dimers can also be exchanged along the filament shaft and that this mechanism of self-repair promotes filament rescue Théry and Blanchoin (2021). The renewal of the tubulin dimers is spontaneous and occurs at lattice defects or damage sites and impacts both microtubule dynamical and mechanical properties Théry and Blanchoin (2021). In the absence of prior defects, estimates of the free energy of a tubulin dimer dissociating from the (intact) microtubule lattice range from 35 to 80 $k_{\mathrm{B}}T$ Schaedel et al. (2019), suggesting that spontaneous exchange of tubulin is negligible over the lifetime of the microtubule (a few minutes). On the contrary, since the lifetime of vimentin filaments is much longer (a few tens of hours) and the free energy of vimentin tetramers much smaller ($\sim$26 $k_{\mathrm{B}}T$, measured here), spontaneous vimentin subunit exchange plays a critical role. We showed here that the mechanism of self-repair is important for regulating filament dynamics, but the link between self-repair and mechanical properties remains to be clearly established.

In this study, we elucidate the molecular mechanism responsible for the fragmentation of vimentin filaments, which takes place over a very long time because the filaments are constantly self-repairing. Thus, our results provide a complete and comprehensive description of vimentin turnover. This mechanism of continuous self-repair may be a general feature of intermediate filaments, further studies will be necessary to uncover this phenomenon with other types of IF. Moreover, since more than 90 diseases have been associated with muta-

tions of IF proteins and most of these mutations impact the ability of filament to assemble, future studies could reveal if these mutations also impact subunit exchange and filament integrity. Overall, our results pave the way for new studies aiming at understanding the regulation of IF dynamics, which plays a crucial role in their cellular functions.

METHODS

Detailed protocols are included in Supporting Information.

Vimentin

We purified recombinant wild-type human vimentin following the protocol from Herrmann et al. Herrmann et al. (2004). We labeled vimentin using Alexa Fluor (AF) 488, AF 568, and AF 647 maleimide dyes that form covalent bonds with the cysteine-328 on vimentin as described previously Tran et al. (2023), Winheim et al. (2011).

Vimentin filament assembly

Vimentin, stored in 8M urea at -80 °C, was renatured by stepwise dialysis from 8 M, 6 M, 4 M, 2 M, 1 M, 0 M urea to sodium phosphate buffer (pH 7.0, 2.5 mM sodium phosphate, 1 mM DTT). We assembled vimentin filaments for all the experiments using a standard 'kick-start' assembly protocol, except specially notified. We added KCl to a solution of vimentin at the desired concentration and labeling rate (typically 0.2 mg/mL with 15% labeling) with a final concentration of 100 mM KCl. Then, the vimentin mixture was incubated at 37 °C for 2 h.

Mixing filament experiment

We assembled two sets of unlabeled and labeled vimentin (AF 488, 15% labeling rate), both at 0.2 mg/mL, at 37 °C for 2 h, then mixed them at a ratio 1:1 or 9:1 and continued to incubate the mixture at 37 °C for 24 h.

Dilution experiment

We diluted pre-assembled filaments (AF 488, 15% labeling rate, 0.2 mg/mL, assembled at 37 °C for 2 h) at dilution ratios 1:200 and 1:500 in the assembly buffer and incubated the diluted samples for another 6 h at 37 °C. For experiments in which filaments were diluted in tetramers, we diluted the pre-assembled filaments in the assembly buffer that was added with vimentin tetramers (at the desired concentration and labeling rate) in advance.

Direct observation of subunit dissociation along immobilized filaments on substrate

We followed a protocol of TIRF microscopy experiment from our previous works Petitjean et al. (2024), Tran et al. (2023). In short, we prepared flow chambers with different heights and coated them with antibodies of AF 488 and passivated by F127. Pre-assembled labeled filaments (AF 488, 15% labeling rate, 0.2 mg/mL, assembled at 37 °C for 2 h) were flowed into the chamber and constrained on substrate. The flow chamber was then flushed with the assembly buffer only to remove unbound filaments and pre-existing subunits. The chamber was sealed and incubated in a microscope stage at 35 °C for 6 h.

ACKNOWLEDGMENT

We thank the Romet-Lemonne/Jegou lab for assistance and exciting discussions, Guillaume Lamour and Clément Campillo for preliminary data acquisition not included in the manuscript, and Ingrid Billault-Chaumartin for careful reading of the manuscript. CL thank Harald Herrmann and Tatjana Wedig for teaching her vimentin purification, and the support of the EU-supported Cooperation in Science and Technology (COST) action NANONET. This project was funded by "Investissements d'Avenir" Labex WhoAmI? (ANR-11-LABX-0071) and the Université Paris Cidé IdEx (ANR-IDEX-0001), LabEx PALM (ANR-10-LABX- 0039-PALM), the Agence Nationale pour la recherche (ANR-21-CE11-0004-02), the Impulscience program of Fondation Bettencourt-Schueller and the Centre National de la

Recherche Scientifique.

Belmont, L. D. and Mitchison, T. J. (1996). Identification of a protein that interacts with tubulin dimers and increases the catastrophe rate of microtubules. *Cell*, 84(4):623–631.

Block, J., Witt, H., Candelli, A., Danes, J. C., Peterman, E. J. G., Wuite, G. J. L., Janshoff, A., and Köster, S. (2018). Viscoelastic properties of vimentin originate from nonequilibrium conformational changes. *Sci. Adv.*

Block, J., Witt, H., Candelli, A., Peterman, E. J., Wuite, G. J., Janshoff, A., and Köster, S. (2017). Nonlinear loading-rate-dependent force response of individual vimentin intermediate filaments to applied strain. *Phys. Rev. Lett.*, 118(4):048101.

Brennich, M. E., Nolting, J.-F., Dammann, C., Nöding, B., Bauch, S., Herrmann, H., Pfohl, T., and Köster, S. (2011). Dynamics of intermediate filament assembly followed in micro-flow by small angle x-ray scattering. *Lab Chip*, 11(4):708–716.

Coleman, T. R. and Lazarides, E. (1992). Continuous growth of vimentin filaments in mouse fibroblasts. *Journal of cell science*, 103(3):689–698.

Eibauer, M., Weber, M. S., Kronenberg-Tenga, R., Beales, C. T., Boujemaa-Paterski, R., Turgay, Y., Sivagurunathan, S., Kraxner, J., Köster, S., Goldman, R. D., et al. (2024). Vimentin filaments integrate low-complexity domains in a complex helical structure. *Nature Structural & Molecular Biology*, pages 1–11.

Eriksson, J. E., He, T., Trejo-Skalli, A. V., Härmälä-Braskén, A.-S., Hellman, J., Chou, Y.-H., and Goldman, R. D. (2004). Specific in vivo phosphorylation sites determine the assembly dynamics of vimentin intermediate filaments. *J. Cell Sci.*, 117(6):919–932.

Forsting, J., Kraxner, J., Witt, H., Janshoff, A., and Köster, S. (2019). Vimentin intermediate filaments undergo irreversible conformational changes during cyclic loading. *Nano Lett.*, 19(10):7349–7356.

Hémonnot, C. Y., Mauermann, M., Herrmann, H., and Köster, S. (2015). Assembly of simple epithelial keratin filaments: deciphering the ion dependence in filament organization. *Biomacromolecules*, 16(10):3313–3321.

Herrmann, H. and Aebi, U. (2016). Intermediate filaments: Structure and assembly. *Cold Spring Harbor Perspect. Biol.*, 8(11):a018242.

Herrmann, H., Häner, M., Brettel, M., Müller, S. A., Goldie, K. N., Fedtke, B., Lustig, A., Franke, W. W., and Aebi, U. (1996). Structure and assembly properties of the intermediate filament protein vimentin: The role of its head, rod and tail domains. *J. Mol. Biol.*, 264(5):933–953.

Herrmann, H., Kreplak, L., and Aebi, U. (2004). Isolation, characterization, and in vitro assembly of intermediate filaments. In *Methods in cell biology*, volume 78, pages 3–24. Elsevier.

Hookway, C., Ding, L., Davidson, M. W., Rappoport, J. Z., Danuser, G., and Gelfand, V. I. (2015). Microtubule-dependent transport and dynamics of vimentin intermediate filaments. *Mol. Biol. Cell*, 26(9):1675–1686.

Hu, J., Li, Y., Hao, Y., Zheng, T., Gupta, S. K., Parada, G. A., Wu, H., Lin, S., Wang, S., Zhao, X., et al. (2019). High stretchability, strength, and toughness of living cells enabled by hyperelastic vimentin intermediate filaments. *Proc. Natl. Acad. Sci.*, 116(35):17175–17180.

Huber, F., Boire, A., López, M. P., and Koenderink, G. H. (2015). Cytoskeletal crosstalk: when three different personalities team up. *Curr. Opin. Cell Biol.*, 32:39–47. Cell architecture.

Inagaki, M., Nishi, Y., Nishizawa, K., Matsuyama, M., and Sato, C. (1987). Site-specific phosphorylation induces disassembly of vimentin filaments in vitro. *Nature*, 328(6131):649–652.

Kalluri, R. and Weinberg, R. A. (2009). The basics of epithelial-mesenchymal transition. *The Journal of Clinical Investigation*, 119(6):1420–1428.

Kaus-Drobek, M., Mücke, N., Szczepanowski, R. H., Wedig, T., Czarnocki-Cieciura, M., Polakowska, M., Herrmann, H., Wysłouch-Cieszyńska, A., and Dadlez, M. (2020). Vimentin s-glutathionylation at cys328 inhibits filament elongation and induces severing of mature filaments in vitro. *The FEBS Journal*, 287(24):5304–5322.

Kraxner, J., Lorenz, C., Menzel, J., Parfentev, I., Silbern, I., Denz, M., Urlaub, H., Schwappach, B., and Köster, S. (2021). Post-translational modifications soften vimentin intermediate filaments. *Nanoscale*, 13(1):380–387.

Kuo, Y.-W., Mahamdeh, M., Tuna, Y., and Howard, J. (2022). The force required to remove tubulin from the microtubule lattice by pulling on its α-tubulin c-terminal tail. *Nature Communications*, 13(1):3651.

Latorre, E., Kale, S., Casares, L., Gómez-González, M., Uroz, M., Valon, L., Nair, R. V., Garreta, E., Montserrat, N., Del Campo, A., et al. (2018). Active superelasticity in three-dimensional epithelia of controlled shape. *Nature*, 563(7730):203–208.

Leduc, C. and Etienne-Manneville, S. (2015). Intermediate filaments in cell migration and invasion: the unusual suspects. *Curr. Opin. Cell Biol.*, 32:102–112.

Lopez, C. G., Saldanha, O., Huber, K., and Köster, S. (2016). Lateral association and elongation of vimentin intermediate filament proteins: A time-resolved light-scattering study. *Proc. Natl. Acad. Sci.*, 113(40):11152–11157.

Lorenz, C., Forsting, J., Schepers, A. V., Kraxner, J., Bauch, S., Witt, H., Klumpp, S., and Köster, S. (2019). Lateral subunit coupling determines intermediate filament mechanics. *Phys. Rev. Lett.*, 123(18):188102.

Lorenz, C., Forsting, J., Style, R. W., Klumpp, S., and Köster, S. (2023). Keratin filament mechanics and energy dissipation are determined by metal-like plasticity. *Matter*, 6(6):2019–2033.

Martínez-Cenalmor, P., Martínez, A. E., Moneo-Corcuera, D., González-Jiménez, P., and Pérez-Sala, D. (2024). Oxidative stress elicits the remodeling of vimentin filaments into biomolecular condensates. *Redox Biology*, 75:103282.

Murray, M. E., Mendez, M. G., and Janmey, P. A. (2014). Substrate stiffness regulates solubility of cellular vimentin. *Molecular biology of the cell*, 25(1):87–94.

Nagle, I., Delort, F., Hénon, S., Wilhelm, C., Batonnet-Pichon, S., and Reffay, M. (2022). The importance of intermediate filaments in the shape maintenance of myoblast model tissues. *Elife*, 11:e76409.

Ndiaye, A.-B., Koenderink, G. H., and Shemesh, M. (2022). Intermediate filaments in cellular mechanoresponsiveness: mediating cytoskeletal crosstalk from membrane to nucleus and back. *Frontiers in cell and developmental biology*, 10:882037.

Ngai, J., Coleman, T. R., and Lazarides, E. (1990). Localization of newly synthesized vimentin subunits reveals a novel mechanism of intermediate filament assembly. *Cell*, 60(3):415–427.

Nöding, B., Herrmann, H., and Köster, S. (2014). Direct observation of subunit exchange along mature vimentin intermediate filaments. *Biophysical journal*, 107(12):2923–2931.

Nunes Vicente, F., Lelek, M., Tinevez, J.-Y., Tran, Q. D., Pehau-Arnaudet, G., Zimmer, C., Etienne-Manneville, S., Giannone, G., and Leduc, C. (2022). Molecular organization and mechanics of single vimentin filaments revealed by super-resolution imaging. *Sci. Adv.*, 8(8):eabm2696.

Omary, M. B., Ku, N.-O., Strnad, P., Hanada, S., et al. (2009). Toward unraveling the complexity of simple epithelial keratins in human disease. *The Journal of clinical investigation*, 119(7):1794–1805.

Patteson, A. E., Vahabikashi, A., Goldman, R. D., and Janmey, P. A. (2020). Mechanical and non-mechanical functions of filamentous and non-filamentous vimentin. *Bioessays*, 42(11):2000078.

Petitjean, I. I., Tran, Q. D., Goutou, A., Kabir, Z., Wiche, G., Leduc, C., and Koenderink, G. H. (2024). Reconstitution of cytolinker-mediated crosstalk between actin and vimentin. *European Journal of Cell Biology*, 103(2):151403.

Schaedel, L., Triclin, S., Chrétien, D., Abrieu, A., Aumeier, C., Gaillard, J., Blanchoin, L., Théry, M., and John, K. (2019). Lattice defects induce microtubule self-renewal. *Nature physics*, 15(8):830–838.

Schween, L., Mucke, N., Portet, S., Goldmann, W. H., Herrmann, H., and Fabry, B. (2022). Dual-wavelength stopped-flow analysis of the lateral and longitudinal assembly kinetics of vimentin. *Biophysic. J*, 121:1–12.

Snider, N. T. and Omary, M. B. (2014). Post-translational modifications of intermediate filament proteins: mechanisms and functions. *Nat. Rev. Mol. Cell Biol.*, 15(3):163–177.

Soellner, P., Quinlan, R. A., and Franke, W. W. (1985). Identification of a distinct soluble subunit of an intermediate filament protein: tetrameric vimentin from living cells. *Proc. Natl. Acad. Sci.*, 82(23):7929–7933.

Sokolova, A. V., Kreplak, L., Wedig, T., Mücke, N., Svergun, D. I., Herrmann, H., Aebi, U., and Strelkov, S. V. (2006). Monitoring intermediate filament assembly by small-angle x-ray scattering reveals the molecular architecture of assembly intermediates. *Proceedings of the National Academy of Sciences*, 103(44):16206–16211.

Théry, M. and Blanchoin, L. (2021). Microtubule self-repair. *Current Opinion in Cell Biology*, 68:144–154.

Tran, Q. D., Sorichetti, V., Pehau-Arnaudet, G., Lenz, M., and Leduc, C. (2023). Fragmentation and entanglement limit vimentin intermediate filament assembly. *Physical Review X*, 13(1):011014.

Van Kampen, N. G. (1992). *Stochastic processes in physics and chemistry*, volume 1. Elsevier.

Winheim, S., Hieb, A. R., Silbermann, M., Surmann, E.-M., Wedig, T., Herrmann, H., Langowski, J., and Mücke, N. (2011). Deconstructing the late phase of vimentin assembly by total internal reflection fluorescence microscopy (tirfm). *PLoS ONE*, 6(4).

Çolakoğlu, G. and Brown, A. (2009). Intermediate filaments exchange subunits along their length and elongate by end-to-end annealing. *J. Cell Biol.*, 185(5):769–777.

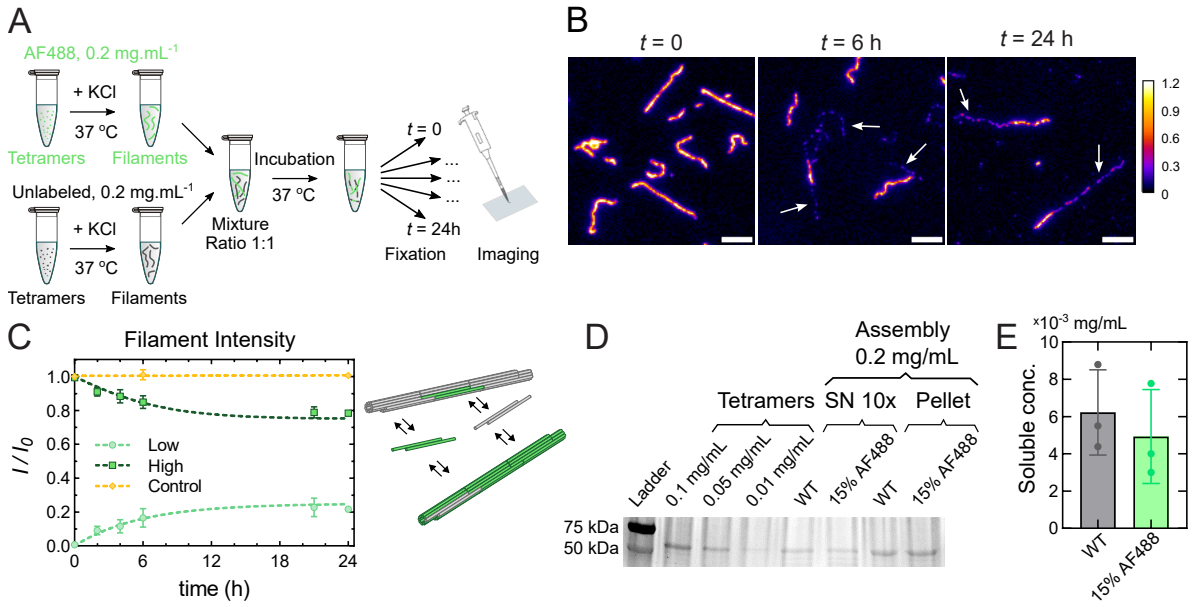

FIG. 1: Exchange of subunits between pre-assembled vimentin filaments. (A) Schematics of the subunit exchange experiment between labeled and unlabeled filaments. Two samples of vimentin filaments were pre-assembled at an initial concentration of 0.2 mg/mL in a phosphate buffer for 2h at 37 °C, one with a 15% AF488 labeling fraction and one without labeling. Filament assembly was triggered by the addition of 100 mM KCL ("kick-start"). The two samples were mixed at time 0 and further incubated at 37 °C for up to 24 h. At different time points after mixing, filaments were diluted 100 times and immediately fixed with 0.25 % glutaraldehyde for imaging. (B) Representative fluorescence images at time 0h, 6h, and 24h after mixing. Colorbar indicates the range of fluorescence intensity normalized by the mean filament intensity at time 0. White arrows indicate segments of filaments that were initially unlabelled. Scale bar: 5 μm. (C) Time evolution of the normalized fluorescence intensity after filament mixing of initially labeled filaments (dark green squares), initially unlabelled filaments (light green circles) and unmixed labeled filaments (yellow diamonds) (see methods). Dashed lines: exponential fit with a characteric rate equal to $k_{\text{off}} = 0.2 \pm 0.1$ h^{-1} (SD, $N = 3$) using Eq. 6 (Sup Info), and linear regression (slope = 0.0001) of the control unmixed filaments. Each data point represents the average over $N = 3$ independent repeats (∼100 filaments per condition and repeat) and the error bars are the standard deviations of the 3 repeats. Right: Schematics depicting the association/dissociation of vimentin subunits along filament shafts. (D) Vimentin concentration measurement through SDS-page gel: (i) 0.1 mg/mL tetramers; (ii) 0.05 mg/mL tetramers; (iii) 0.02 mg/mL tetramers; (iv) 10× supernatant of WT vimentin assembled at 0.2 mg/mL, (v) 10× supernatant of vimentin labeled with 15 % AF488 assembled at 0.2 mg/mL, (vi) pellet of WT vimentin assembled at 0.2 mg/mL, (vii) pellet of vimentin labeled with 15 % AF488 assembled at 0.2 mg/mL. Vimentin filaments were assembled at different concentrations, centrifuged at 140,000 $\times g$ for 15 min and the supernatant was concentrated 10 times and compared with a range of known concentrations. (E) Concentration of vimentin soluble pool, quantified from SDS-page gels. $N = 3$ independent repeats. Error bars are standard deviations.

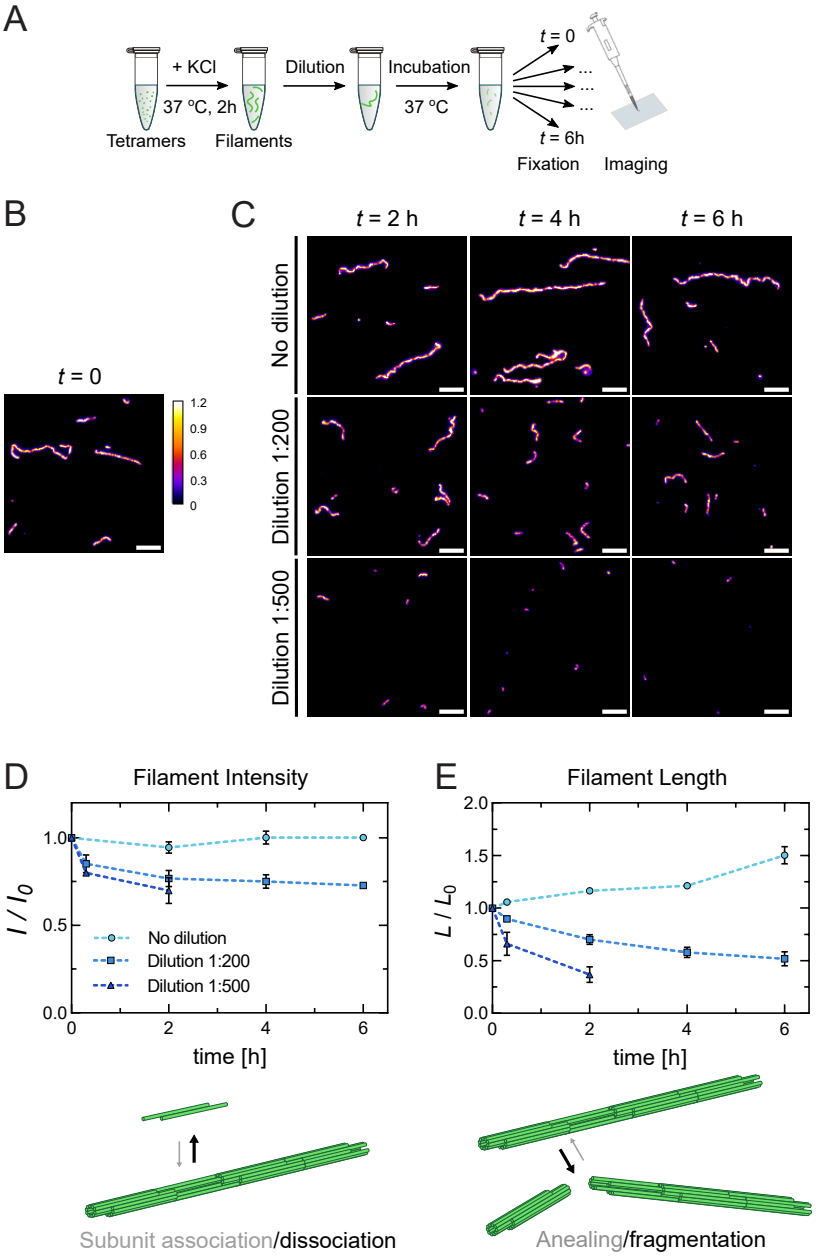

FIG. 2: Dilution induces both filament thinning and filament fragmentation. (A) Schematics of the dilution experiments. Vimentin filaments with 15% AF488 labeling fraction were pre-assembled at an initial concentration of 0.2 mg/mL for 2h at 37 °C. The obtained filaments were then diluted in the assembly buffer at ratios of 1:200 and 1500, and further incubated at 37 °C for up to 6 h. Filaments were fixed with 0.25% glutaraldehyde at different time points after dilution. (B) Representative fluorescence image at time 0, just after dilution 1:200, used as a reference for fluorescence intensity measurements. Scale bar: 5 µm. (C) Representative fluorescence images at time 2h, 4h, and 6h without dilution, after 1:200 and 1:500 dilution. Images were acquired in similar microscopy conditions as in A, and are displayed with the same color scale. Scale bar: 5 µm. (D) Time evolution of the normalized fluorescence intensity of non-diluted filaments (light blue circles), filaments diluted 1:200 (blue squares) and 1:500 (dark blue triangles). Bottom: cartoon illustrating the unbalanced subunit dissociation associated with the decrease in filament intensity. Filaments diluted 1:500 cannot be detected beyond two hours. (E) Time evolution of the mean length of non-diluted filaments (orange circles), filaments diluted 1:200 (red squares) and 1:500 (dark red triangles). Bottom: cartoon illustrating the unbalanced filament fragmentation associated with the decrease in filament length. Each data point of (D) and (E) represents the average of $N = 3$ independent repeats (∼300 filaments per condition and repeat) and the error bars are standard deviations of 3 repeats.

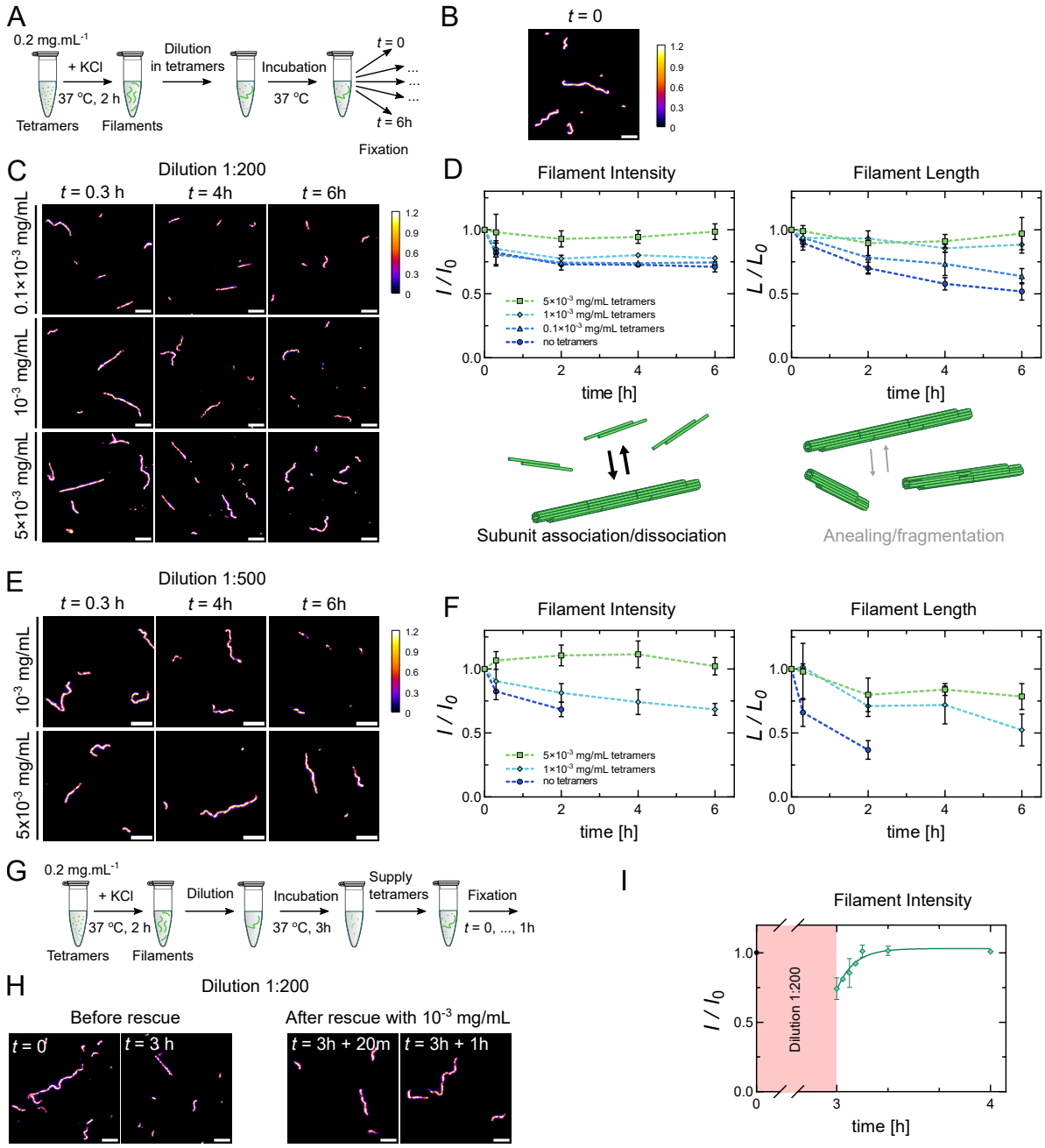
A
0.2 mg.mL-1
+ KCl
37 °C, 2 h
Tetramers
Filaments
Dilution in tetramers
Incubation
37 °C
t = 0
t = 6h
Fixation
B
t = 0
C
Dilution 1:200
t = 0.3 h
t = 4h
t = 6h
0.1×10-3 mg/mL
10-3 mg/mL
5×10-3 mg/mL
D
Filament Intensity
Filament Length
I / I0
L / L0
time [h]
5×10-3 mg/mL tetramers
1×10-3 mg/mL tetramers
0.1×10-3 mg/mL tetramers
no tetramers
Subunit association/dissociation
Anealing/fragmentation
E
Dilution 1:500
F
G
Supply tetramers
t = 0, ..., 1h
H
Before rescue
After rescue with 10-3 mg/mL
t = 3 h
t = 3h + 20m
t = 3h + 1h
I
Dilution 1:200

FIG. 3: Adding soluble tetramers protect diluted filaments from fragmentation. (A) Schematics of the dilution experiments in tetramers. Pre-assembled vimentin filaments (0.2 mg/mL assembled for 2h at 37 °C) were diluted in a solution containing AF-488-labeled vimentin tetramers at different concentrations in the assembly buffer (0.1×10^{-3}, 1×10^{-3}, and 5×10^{-3} mg/mL). The mixtures were incubated at 37 °C for up to 6 h. Filaments were fixed with 0.25% glutaraldehyde at different time points after dilution. (B) Representative fluorescence image at time 0, just after dilution 1:200, used as a reference for fluorescence intensity measurements. Scale bar: 5 µm. (C) Representative fluorescence images at time 0.3h, 4h, and 6h after 1:200 dilution in a 0.1×10^{-3}, 1×10^{-3}, and 5×10^{-3} mg/mL vimentin solution. Scale bar: 5 µm. (D) Time evolution of the normalized fluorescence intensity (left) and mean filament length (right) of filaments diluted 1:200 in a solution without tetramers (circles), with 0.1×10^{-3} mg/mL (triangles), 10^{-3} mg/mL (diamonds) and 5×10^{-3} mg/mL (squares). Bottom: cartoon illustrating the subunit dissociation balanced by subunit association when filaments are diluted in a 5×10^{-3} mg/mL vimentin tetramer solution, preventing filament thinning. (E) Fluorescence images at time 2h, 4h, and 6h after 1:500 dilution in a 10^{-3} and 5×10^{-3} mg/mL vimentin solution. Scale bar, 5 µm. Bottom: cartoon illustrating that filament fragmentation and end-to-end annealing are balanced when filaments are diluted in a 5×10^{-3} mg/mL solution of tetramers leading to the absence of filament shortening. (F) Time evolution of the normalized fluorescence intensity (left) and mean filament length (right) of filaments diluted 1:500 in a solution without tetramers (circles), with 10^{-3} mg/mL (diamonds) and 5×10^{-3} mg/mL (triangles). (G) Schematics of filament rescue experiment. Pre-assembled filaments were first diluted 1:200 for 3 h, then supplied with 10^{-3} mg/mL AF-488-labeled tetramers. (H) Representative fluorescence images at time 0h and 3h after dilution, and time 20 min and 1 h after the addition of 10^{-3} mg/mL tetramers. Scale bar: 5 µm. (I) Time evolution of the normalized fluorescence intensity of filaments to time 0, diluted 1:200 for 3h and then for 2h after the addition of $c = 10^{-3}$ mg/mL of tetramers. Solid line: fit by an exponential with a characteristic rate equal to $k_{\mathrm{on}}.c$ up to 1h after addition of tetramer (see Theoretical modeling in the methods section) Each data point of (B), (C) and (H) represents the average of $N = 3$ independent repeats (∼300 filaments per condition and repeat) and the error bars the standard deviation of the 3 repeats.

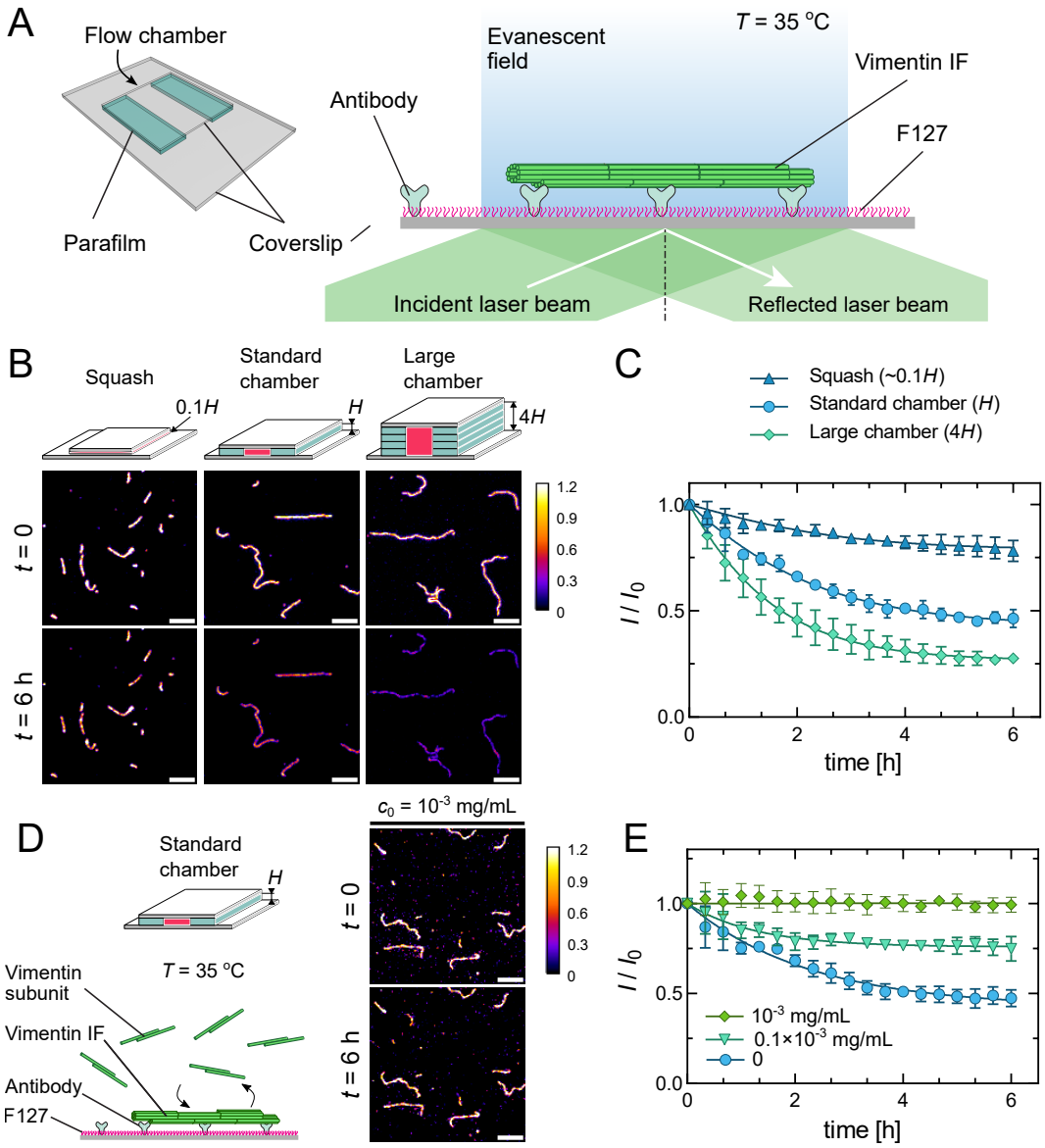
A
Flow chamber
Parafilm
Coverslip
Antibody
Evanescent field
T = 35 °C
Vimentin IF
F127
Incident laser beam
Reflected laser beam
B
Squash
Standard chamber
Large chamber
0.1H
H
4H
t = 0
t = 6 h
1.2
0.9
0.6
0.3
0
C
Squash (~0.1H)
Standard chamber (H)
Large chamber (4H)
I / I0
time [h]
D
Standard chamber
H
T = 35 °C
Vimentin subunit
Vimentin IF
Antibody
F127
c0 = 10-3 mg/mL
t = 0
t = 6 h
E
10-3 mg/mL
0.1×10-3 mg/mL
0
I / I0
time [h]

FIG. 4: Direct observation of subunit dissociation along filaments after dilution. (A) Schematics of the TIRF microscopy setup for *in situ* filament dilution experiments in a flow chamber. AF-488 labeled pre-assembled vimentin filaments (assembly of 0.2 mg/mL for 2h at 37 °C) were diluted and flushed into a flow chamber made of silanized coverslips, where they can attach to the substrate decorated with anti-AF488 antibodies and passivated by F127. The chamber was rinsed with the assembly buffer to remove all unwanted vimentin subunits, then sealed and incubated at ∼35 °C. (B) Schematics of the flow chambers with 3 different chamber heights (0.1H, H and 4H, with H being the thickness of the standard chamber assembled with one layer of parafilm), and representative fluorescence images of filaments at the same observation region, at time 0 vs. 6h. Scale bar: 5 µm (C) Time evolution of the mean fluorescence intensity of filaments normalized by the value at time 0 and for different chamber heights: $0.1H$ (dark blue triangle), H (light blue circles), and $4H$ (green diamonds). Solid line: fit using equation 6 of the supplementary material. (D) Schematics of the TIRF microscopy setup for *in situ* filament dilution in the standard chamber containing different concentrations of AF-488-labeled tetramers (left). Representative fluorescence images of filaments submerged in 10^{-3} mg/mL tetramers at the same observation region, at time 0 vs. 6 h. Scale bar: 5 µm. (E) Time evolution of the mean fluorescence intensity normalized by the value at time 0, after dilution in the assembly buffer without tetramers supplied (blue circles) and after dilution in a solution of 0.1×10^{-3} (light green triangles) and 10^{-3} mg/mL (green diamonds) labeled tetramers. Each data point of (C) and (E) represents the average of $N = 3$ independent repeats (∼50 filaments per condition and repeat) and the error bar the standard deviation of the 3 repeats.

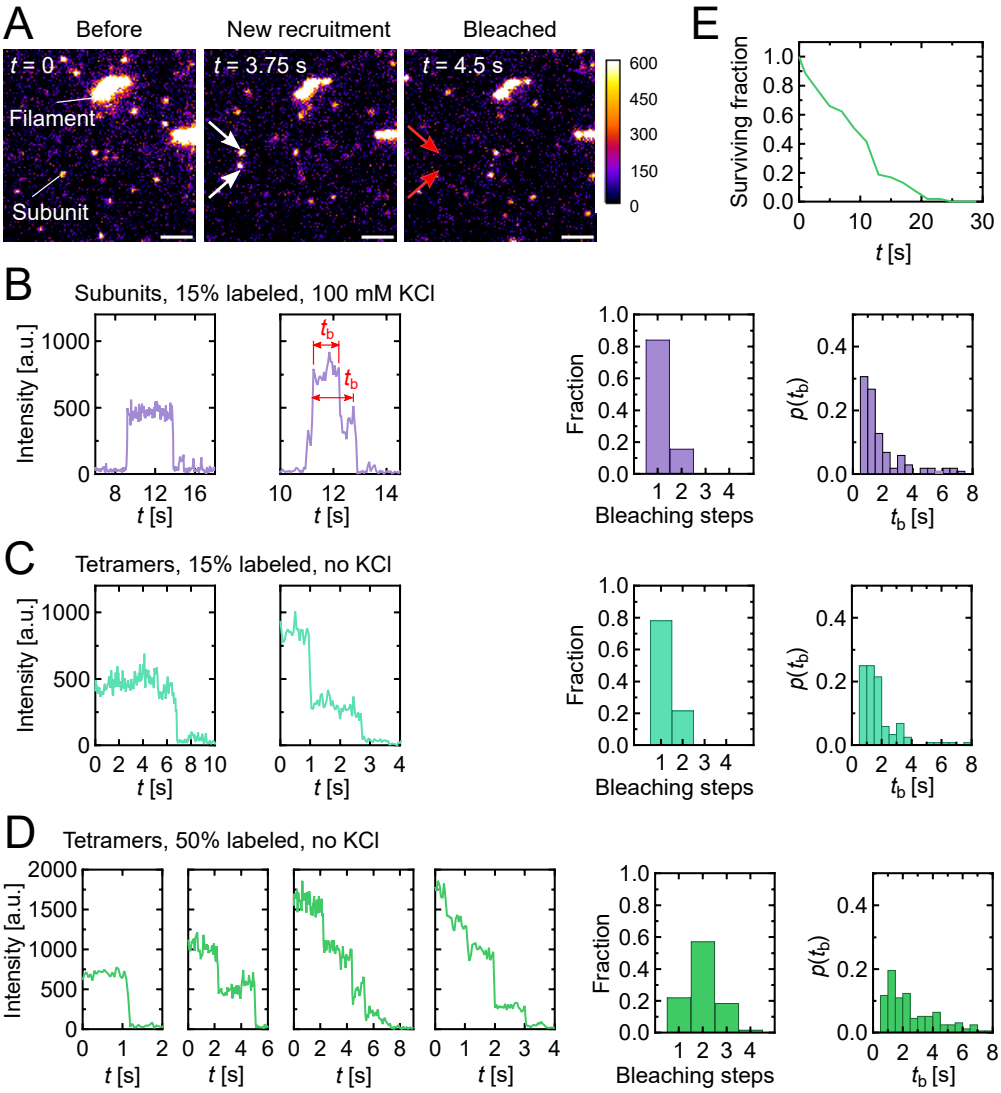

FIG. 5: Exchanged subunits are tetramers. (A) Representative fluorescence images of vimentin subunits during bleaching experiments. Pre-assembled filaments (assembly of 0.2 mg/mL for 2h at 37 °C) were introduced to a flow chamber and immobilized on the substrate using the same setup as in Fig. 4A. The flow chamber was rinsed with the assembly buffer to remove all remaining vimentin subunits, then sealed and maintained at ∼37 °C. High-power laser was applied to quickly bleach all the subunits dissociating from the filaments and binding to the substrate. White arrows indicate newly recruited subunits on the surface, red arrows indicate the positions of photobleached subunits. Color scale indicates the fluorescence intensity. Scale bar: 2 µm. B-D) Left : examples of fluorescence bleaching steps, middle: distribution of bleaching steps per spot; right: distribution of bleaching times (t_b), in three conditions: (B) 15% labeled vimentin subunits dissociated from filaments, in assembly buffer; (C) 15% and (D) 50% labeled vimentin tetramers, in buffer lacking KCl. Distributions of bleaching steps and durations were obtained from a sample size of ∼200 spots for each condition. E) Fraction of subunits detached from the surface quantified at a low-power laser. The distribution was obtained from 65 subunits.

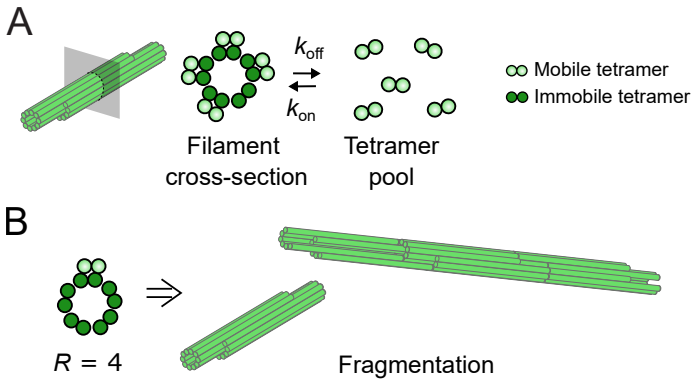

FIG. 6: Kinetic scenario for filament fragmentation. (A) Model of the two tetramer populations (mobile and immobile) existing in the vimentin filament structure. Immobile tetramers form an inner core, while mobile tetramers form an outer layer and can associate/dissociate with association rate k_{on} and dissociation rate k_{off}. Adjacent tetramers of the outer layer are connected through their tail domains which are not represented in this simplistic cartoon. The exact position of the immobile tetramers within the filament structure is unknown and is hypothetically represented here as an inner layer. (B) Mechanism of filament fragmentation: fluctuations in the number of tetramers per cross-section lead to fragmentation. When the number of mobile tetramers removed reaches the critical value, $R = 4$, the filament breaks at this location.